FLEXURAL PERFORMANCE ON RC AND PRECAST CONCRETE COLUMNS WITH ULTRA HIGH STRENGTH MATERIALS UNDER VARYING AXIAL LOAD

Toshio Matsumoto[1], Hiroshi Nishihara[1] and Masato Nakao[2]

[1] *Technical Research Institute, Ando Corporation,1-19-61, Oichuo, Fujimino, Saitama, 356-0058, JAPAN*
[2] *Research Associate, Faculty of Engineering, Yokohama National University, Kanagawa, 240-8501, JAPAN*
Email: [1]LDZ06301@nifty.com, [2] mnakao@ynu.ac.jp

ABSTRACT :

In this experimental study, it was clarified the structural performance of reinforced concrete (RC) and precast concrete (PCa) columns with ultra-high-strength materials. Anti-symmetrical cyclic lateral loads and varying axial loads corresponding to the axial load acting on the exterior column in lower story were applied to the column specimens. The alternative of the design standard strength (F_c) of the concrete is 80 MPa and 120 MPa, and the nominal yield strength of the main reinforcing bar is 490 MPa and 685 MPa. The nominal yield strength of shear reinforcement in a column is 1275 MPa. The six column specimens were manufactured with the combinations of such materials.
The flexural capacity obtained from the experiment was evaluated using the equation of Building Code and Commentary ACI 318-02(2002), and it was found that the equation overestimated the flexural capacity for the F_c 120 MPa specimen. Therefore, the flexural capacity of each specimen was reevaluated using rectangular stress blocks designed for high-strength concrete.

KEYWORDS: ultra-high-strength material, reinforced concrete column, precast concrete column, varying axial load, flexural performance, evaluation of capacity.

1. INTRODUCTION

In recent years, RC buildings are becoming super-high-rise and long-span structures. In such buildings, the columns of the lower stories are subjected to large long-term axial loads. Moreover, when an earthquake occurs, a large varying axial load acts on the exterior columns. Therefore, it is necessary to use higher strength concrete and reinforcing bars, and also the use of more PCa members to rationalize the construction of such super-high-rise buildings in shorter work periods is inevitable.
Six specimens which consist of RC and PCa columns, were manufactured by combining concrete design nominal strength (F_c) 80 MPa and 120 MPa, nominal yield strength of the longitudinal reinforcements 490 MPa (SD490) and 685 MPa (USD685), and nominal yield strength of shear reinforcement 1275 MPa (SBPD1275). This study aimed to clarify the flexural performance of column members made of ultra-high-strength materials by conducting a static bending shear force test on specimens of external columns in the lower stories subjected to varying axial load.
Furthermore, the flexural capacity obtained from the experiment was evaluated to determine whether or not the rectangular stress block method in accordance with the equation of Building Code and Commentary ACI 318-02 (2002) , which was designed for normal-strength concrete, is applicable to high-strength concrete such as the specimens used in this study.

2. EXPERIMENTAL PROGRAM

2.1. Description of Specimens

Table 2.1 shows the structural specifications of each specimen. The six specimens have an area of 330 (width:

b) x 330 (overall depth: D) (mm) which is equivalent to 1/3 of the actual column cross-sectional area and a shear span ratio ($M/(V{\cdot}D)$) of 2.0 in consideration of flexural failure. As shown in Table 2.1, the specimens are roughly divided into three specimens of F_c 80 MPa and another three specimens of F_c 120 MPa. The values of longitudinal reinforcements 16-D22(# 7) (Grade: SD490) and 16-D19(# 6) (Grade: USD685) for monolithic cast RC column members with respect to each F_c value, and full-PCa column members of the latter value of 16-D19 (USD685) were taken into consideration as the variable factors of the specimens. Four of the 16 longitudinal reinforcements are core reinforcing bars for use in exterior columns in the lower stories. The lateral ties (hoops), used commonly in all the specimens, were small-diameter deformed PC steel bars arranged in a single-stroke enclosed lattice pattern.
The specimens 'C80D22' and 'C80D19' shown in Table 2.1 have different ratios of total area of longitudinal reinforcements to the gross area of column concrete cross-section (A_{st}/A_g) but their calculated flexural strengths are almost the same. On the other hand, the specimen 'PC80D19' uses a mortar-filled splice sleeve joint to join the longitudinal reinforcements in both column base and capital. The hoops used in these joint sections are the same as those used in other sections. The specimens 'C120D22', 'C120D19' and 'PC120D19' have the same structural specifications as the specimens 'C80D22', 'C80D19', and 'PC80D19' respectively, except for their F_c being 120 MPa. Figure 2.1 shows the shapes of specimens and their bar arrangement.
Table 2.2 shows the mechanical properties of the reinforcements used in this experiment. Table 2.3 shows the mechanical properties of the concrete. The concrete materials for the specimens include high-early-strength Portland cement for F_c 80 MPa and normal Portland cement for F_c 120 MPa with about 10 WT% of silica fume as admixture. Crushed stones having the maximum diameter of 13 mm were used as coarse aggregate for all.

Table 2.1 Structural specifications of test specimens.

Specimen	Longitudinal reinforcement A_{st}/A_g (%)	Concrete F_c (MPa)	Hoop (PC steel bar) p_h (%)	Varying axial load P
C80D22	16-D22(SD490) 5.69%	F_c 80	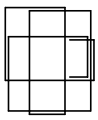 4-RB6.2 @50 (SBPD 1275/1420) 0.73%	Compressive: $+0.55F_cbD$ $(+0.50F_cbD)$* ⇕ Tensile: $-0.7A_{st}f_y$
C80D19	16-D19(USD685)			
PC80D19	4.22%			
C120D22	16-D22(SD490) 5.69%	F_c 120		
C120D19	16-D19(USD685)			
PC120D19	4.22%			

*$0.50F_cbD$ in the case of F_c 120 MPa.
b (width)=330mm
D (overall depth)=330mm
h (clear height)=1320mm
$M/(VD)$ (shear span ratio)=2.0

Table 2.2 Mechanical properties of reinforcements.

Bar size	f_y MPa	ε_y	f_t MPa	E_s GPa	Elongation %
D22(#7)(SD490)	522	0.0028	715	196	17
D19(#6)(USD685)	745	0.0057	1008	202	12
Hoop: RB6.2(#2) (SBPD1275/1420)	1275*	0.0077	1442	198	7

*Taken as the 0.2% proof stre
f_y = yield strength
ε_y = yield strain
f_t = tensile strength
E_s = elastic modulus

Table 2.3 Mechanical properties of concrete and mortar.

Specimen	f_c' MPa	E_c GPa	$_cf_t$ MPa	Specimen	f_c' MPa	E_c GPa	$_cf_t$ MPa
C80D22	92.4	37.4	5.95	C120D22	135.6	44.3	7.44
C80D19	98.4	38.7	5.48	C120D19	136.0	44.3	6.91
PC80D19	98.7	39.4	5.00	PC120D19	134.4	44.3	6.80
J. mortar*	136.6	41.4	—	J. mortar*	147.8	43.6	—

*Joint mortar and grout.
f_c' =concrete cylinder compressive strength
E_c =elastic modulus
$_cf_t$ =splitting strength

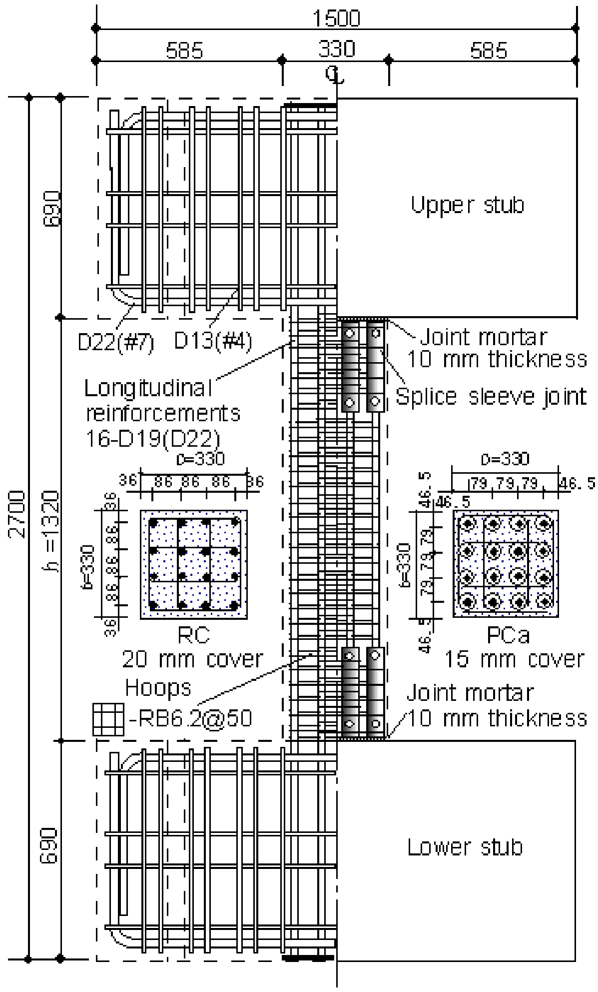

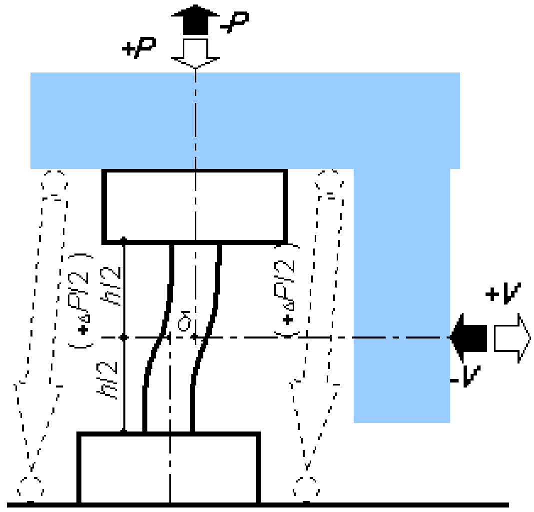

Figure 2.2 Anti-symmetrical loading system.

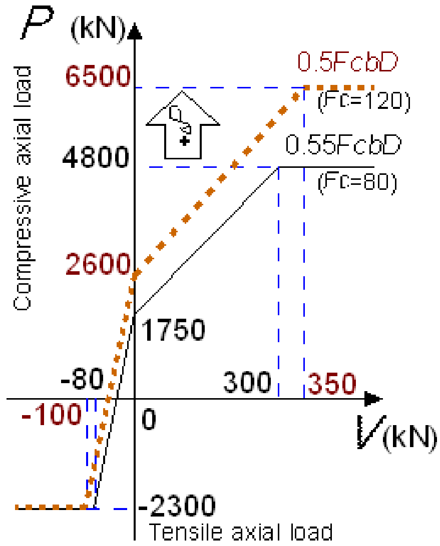

Figure 2.1 Dimensions of specimens. (All dimensions in mm)

Figure 2.3 Loading method of varying axial load.

2.2. Test Setup and Loading Sequence

For loading specimens, an L-shaped loading beam as shown in Figure 2.2 was used. While varying axial load was applied to the specimen, anti-symmetric static bending shear force, with the center level of the clear height being the point of contraflexure, was also applied to the specimen repeatedly, with positive and negative horizontal shear forces applied alternately.

Figure 2.3 shows the loading method of varying axial load, where the compressive axial load is expressed as positive load. First, long-term compressive axial load of $0.2F_cbD$ was applied. Then, axial load (P) was gradually changed in accordance with the horizontal shear force (V). The upper limit and lower limit of the axial load were the compressive axial load $0.55F_cbD$ ($0.50F_cbD$ in the case of F_c 120 MPa) in positive shear force loading and the tensile axial load $-0.7A_{st}\,f_y$ ($A_{st}\,f_y$: product of the total area of the longitudinal reinforcements and the actual yield strength) in negative shear force loading. The axial load was kept constant thereafter.

The horizontal shear force was controlled on the basis of story drift angle ($R = \delta/h$, δ:relative horizontal displacement between upper and lower stubs, h:clear height of column). The experiment was terminated after applying shear force once at $R = \pm 2.5/1000$, twice at $R = \pm 5/1000$, $\pm 10/1000$, $\pm 15/1000$, and $\pm 20/1000$, and once at $R = \pm 30/1000$ and $+50/1000$ respectively.

3. DISCUSSION OF TEST RESULTS

3.1. Outline of the Results

Figure 3.1 shows the relationship between the shear force (V) and story drift angle (R) of all specimens with P-Δ effect taken into consideration. The single-dot chained lines in the Figure 3.1 represent the proof strength in the case where the hysteretic curve with P-Δ effect taken into consideration is lowered to a level that is 95% of the maximum shear force. Table 3.1 shows the shear strength and story drift angle of each loading. The shear strength values in the Table 3.1 are those with P-Δ effect taken into consideration, except for the "first cracking".

Photo 3.1 shows the final conditions (R = +50/1000) of the specimens. The failure patterns shown in Photo 3.1 show flexural crushing in the column capital and column base of the specimens. With the PCa column specimens 'PC80D19' and 'PC120D19', the degree of shear cracking in the central area of the test section and crushing from the joints to the positions just above the joints was remarkable. However, no such phenomena as buckled longitudinal reinforcements and rupture of hoops were observed in any specimen.

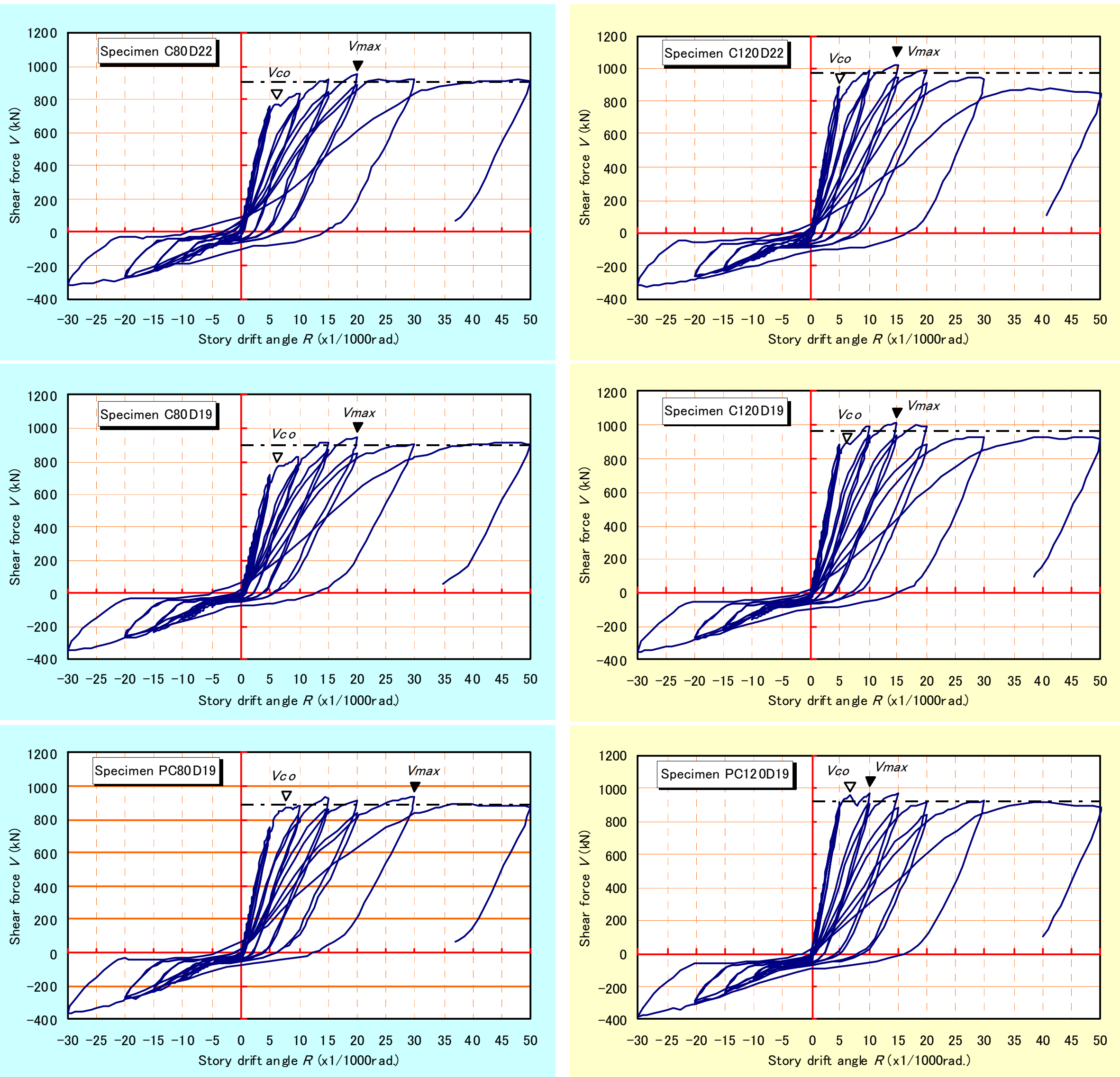

Figure 3.1 Relationship between the shear force (V) and story drift angle (R).

Table 3.1 Experimental results of specimens.

Specimen	*fc'* MPa	±	*Vcr* kN	*Rcr* x1/1000	*Vy* kN	*Ry* x1/1000	*Vco* kN	*Rco* x1/1000	*Vmax* kN	*Rmax* x1/1000	*Vul* kN	*Rul* x1/1000
C80D22	92.4	+	—	—	755.5	5.47	774.7	5.92	948.9	20.05	909.5	50.07
		-	-51.9	-0.73	-75.4	-4.58	—	—	-325.4	-30.02	-325.4	-30.02
C80D19	98.4	+	—	—	786.2	9.99	770.3	6.48	938.8	20.02	900.5	50.03
		-	-37.9	-0.48	-159.3	-9.70	—	—	-347.4	-29.64	-347.4	-29.64
PC80D19	98.7	+	—	—	838.6	10.93	870.5	7.61	935.1	29.26	873.4	50.03
		-	-37.9	-0.50	-148.0	-9.42	—	—	-360.9	-29.33	-360.9	-29.33
C120D22	135.6	+	—	—	877.0	4.78	888.0	5.00	1022.7	15.03	849.5	50.10
		-	-54.9	-0.58	-89.8	-5.02	—	—	-326.2	-28.37	-326.2	-28.37
C120D19	136.0	+	—	—	972.5	12.08	892.0	6.08	1013.4	15.01	912.1	50.05
		-	-56.9	-0.61	-188.2	-12.74	—	—	-353.2	-30.02	-353.2	-30.02
PC120D19	134.4	+	—	—	897.1	7.96	955.1	6.73	968.8	10.02	881.1	50.17
		-	-53.9	-0.45	-123.3	-7.60	—	—	-385.2	-30.04	-385.2	-30.04

fc' = concrete cylinder compressive strength
Vcr (*Rcr*) = shear strength (drift angle) at the first cracking
Vy (*Ry*) = shear strength (drift angle) at the yield of longitudinal reinforcement
Vco (*Rco*) = shear strength (drift angle) at the spalling of cover concrete (1st peak)
Vmax (*Rmax*) = shear strength (drift angle) at the maximum horizontal force (2nd peak)
Vul (*Rul*) = shear strength (drift angle) at the final drift angle

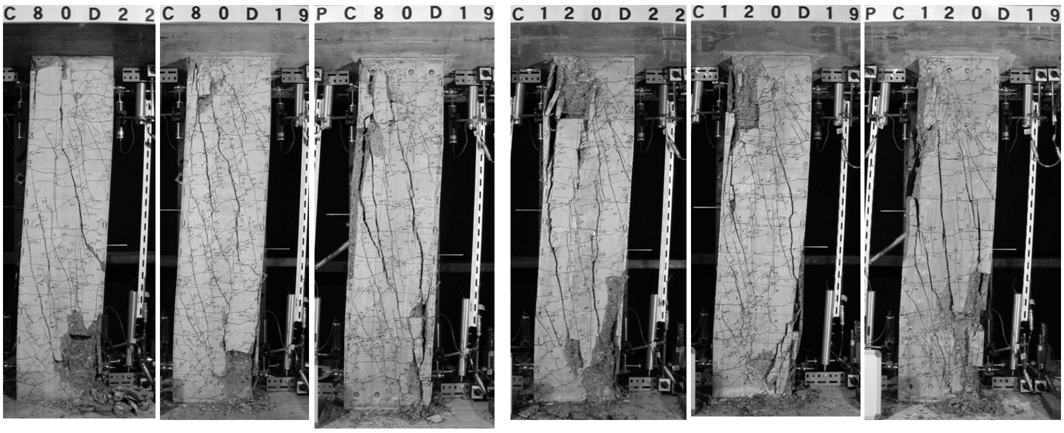

Photo 3.1 Final conditions (R = +50/1000) of specimens.

3.2. Strains in Axial Direction

Figure 3.2 shows the relationship between the axial strain and story drift angle of each specimen. For the expression of the axial strains, the elongation displacement between upper and lower stubs at the axial position in the column was divided by the clear height of column (h) and the tensile strain was expressed as a positive value. The strain performance in the axial direction of the F_c 80 MPa and F_c 120 MPa specimens while applying tensile axial load remained almost the same. The axial strains of the F_c 120 MPa specimen during the large deformation period at and after R = +10/1000 in compressive axial load application mode became large. Also from the appearance of final condition shown in Photo 3.1, it is clear that the degree of crushing in the F_c 120 MPa specimen is larger than that in the F_c 80 MPa specimen, together with spalling of cover concrete over a larger surface area of the F_c 120 MPa specimen.

According to the equation of Building Code and Commentary ACI 318-02 (2002), the axial compressive capacity of a column member using normal-strength concrete is given by the following Eqn. 3.1.

$$P_0 = 0.85 f_c'(A_g - A_{st}) + A_{st} f_y \tag{3.1}$$

In connection with Eqn. 3.1 above, Ozbakkaloglu and Saatcioglu (2004) proposed the following equation as an axial compressive capacity expression applicable to a column using concrete of strengths from normal to high-strength level (120 MPa).

$$P_{0\,(HSC)} = 0.9\, k_4\ f_c'\, (A_g - A_{st}) + A_{st}\, f_y \tag{3.2}$$
$$k_4 = \gamma + (1-\gamma)\, A_c / A_g \ \leq\ 0.95 \tag{3.3}$$
$$\gamma = 1.1 - 0.007\, f_c' \leq\ 0.8 \tag{3.4}$$

Table 3.2 shows the axial compressive capacity of each specimen obtained by using Eqns. 3.1 and 3.2. The rate of loaded axial force, which is obtained by dividing the compressive axial load (P) applied to each specimen by the product of the compressive strength of concrete (f_c') and total cross-sectional area of the column (A_g), is slightly larger in the F_c 80 MPa specimen than in the F_c 120 MPa specimen. However, calculation of the ratios of axial compressive capacity (P_0), based on Eqns. 3.1 and 3.2, to the loaded axial force (P) resulted in a clearly greater ratio for the F_c 120 MPa specimen in Eqn. 3.2 than in Eq. 3.1 of ACI 318-02 (2002). It is safe to assume that this greater ratio caused the increase in the axial strains of the F_c 120 MPa specimen during the large story drift angle. There was no difference in the axial strains between RC column specimens prepared by monolithic casting and PCa column specimens.

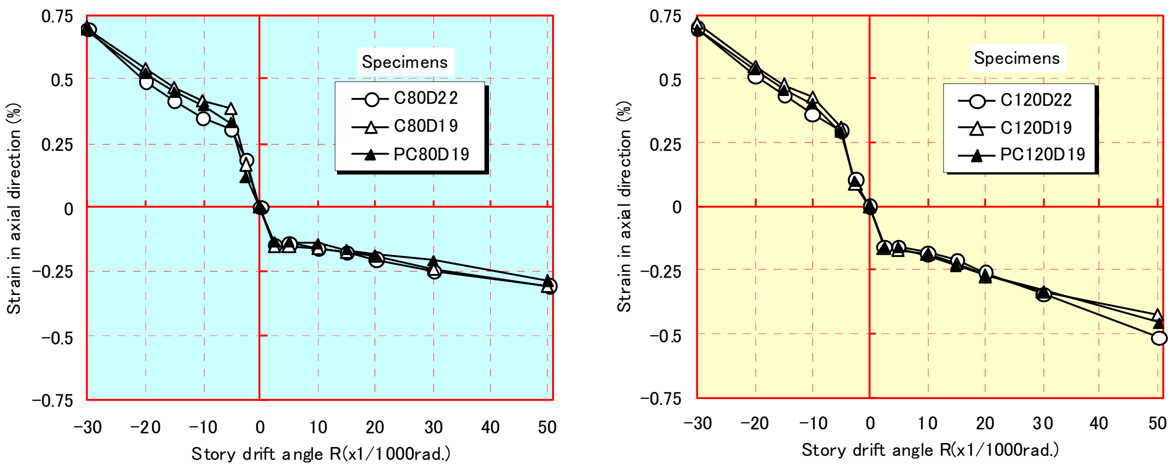

Figure 3.2 Relationship between the strain in the axial direction and story drift angle.

Table 3.2 Axial compressive capacity of specimens.

Specimen	fc' MPa	Ag mm²	Ac mm²	Ast mm²	P kN	P/(fc'Ag)	P_0 kN	P/P_0	mean	$P_{0(HSC)}$ kN	$P/P_{0(HSC)}$	mean
C80D22	92.4	108900	80656	6192	4800	0.477	11299	0.425	0.405	10562	0.454	0.442
C80D19	98.4		80656	4592		0.448	12145	0.395		11248	0.427	
PC80D19	98.7		71824	4592		0.447	12172	0.394		10823	0.444	
C120D22	135.6	108900	80656	6192	6500	0.440	15070	0.431	0.425	13006	0.500	0.503
C120D19	136.0		80656	4592		0.439	15479	0.420		13367	0.486	
PC120D19	134.4		71824	4592		0.444	15337	0.424		12426	0.523	

P = upper limit of the compressive axial load
P_0 = nominal concentric compressive capacity, defined in Eqn. 3.1
$P_{0(HSC)}$ = nominal concentric compressive capacity, defined in Eqn. 3.2

4. EVALUATION OF FLEXURAL CAPACITY

The experimental shear strength values for spalling of cover concrete and maximum shear force (referred to also as "first peak: *Vco*" and "second peak: *Vmax*") shown in Table 3.1 were compared with calculated values respectively, as shown in Table 4.1.

The calculated values, with respect to the coefficients (α_1 and β_1) which constitute the rectangular stress block, were based on both (i) Equation of Building Code and Commentary ACI 318-02 (2002) and (ii) Equation proposed by Ozbakkaloglu and Saatcioglu (2004).

The coefficients α_1 and β_1 represented by both (i) and (ii) at a compressive strength of concrete $f_c' \geq 30$ MPa are shown below. The ultimate compressive strain at extreme fiber (ε_u) is 0.003 in common.

(i) Equation of Building Code and Commentary ACI 318-02 (2002)

$$\alpha_1 = 0.85 \tag{4.1}$$
$$\beta_1 = 0.85 - 0.008\,(f_c' - 30) \geq 0.65 \tag{4.2}$$

(ii) Equation proposed by Ozbakkaloglu and Saatcioglu (2004)

$$\alpha_1 = 0.85 - 0.0014\,(f_c' - 30) \geq 0.72 \tag{4.3}$$
$$\beta_1 = 0.85 - 0.0020\,(f_c' - 30) \geq 0.67 \tag{4.4}$$

Table 4.1 Comparison of experimental and calculated flexural capacity values.

Specimen	*P-Δ* effect	*Vco* kN	*Vmax* kN	V_{ACI} kN	1st Vco/V_{ACI}	2nd $Vmax/V_{ACI}$	V_{HSC} kN	1st Vco/V_{HSC}	2nd $Vmax/V_{HSC}$
C80D22	no	746.3	853.1	726.8	1.03	1.17	727.4	1.03	1.17
	yes	774.7	948.9		1.07	1.31		1.07	1.30
C80D19	no	739.3	843.1	720.5	1.03	1.17	704.4	1.05	1.20
	yes	770.3	938.8		1.07	1.30		1.09	1.33
PC80D19	no	834.1	857.1	697.2	1.20	1.23	680.6	1.23	1.26
	yes	870.5	935.1		1.25	1.34		1.28	1.37
C120D22	no	855.3	924.8	968.6	0.88	0.95	858.8	1.00	1.08
	yes	888.0	1022.7		0.92	1.06		1.03	1.19
C120D19	no	852.4	929.6	930.5	0.92	1.00	819.6	1.04	1.13
	yes	892.0	1013.4		0.96	1.09		1.09	1.24
PC120D19	no	911.1	903.7	896.9	1.02	1.01	788.2	1.16	1.15
	yes	955.1	968.8		1.06	1.08		1.21	1.23

V_{ACI} = flexural capacity calculated by Equation of ACI 318-02 (2002)
V_{HSC} = flexural capacity calculated by Equation of Ozbakkaloglu and Saatcioglu (2004)

The experimental shear strength values of both the first and second peak were evaluated with respect to the case where *P-Δ* effect was taken into consideration as well as the case where *P-Δ* effect was not taken into consideration. According to Table 4.1, the experimental shear strength values of both the first and second peak of F_c 80 MPa specimens are higher than the calculated values determined by Eqns. (i) and (ii) even in the case where *P-Δ* effect is not taken into consideration. Because the calculated shear strength values determined by Eqns. (i) and (ii) were based on the assumption that ε_u is 0.003 equally, the shear strength from the first peak, or spalling of the cover concrete, seems to have been included. Table 4.1 also indicates that the calculated values of the specimens 'C80D22' and 'C80D19' are almost equal to the experimental values of shear strength during the first peak. The experimental shear strength values rose thereafter, too. This means that the second peak, or the shear strength under the maximum load, has a safety factor that is about 1.2 times the values calculated from Eqns. (i) and (ii), even in the case where *P-Δ* effect is not taken into consideration and that the equations can be employed in the structural design.
Regarding the F_c 120 MPa specimens, the experimental shear strength values during the first and second peak, on the basis of the values calculated by Eqn. (i) of Building Code and Commentary ACI 318-02 (2002), cannot be evaluated to be on the safe side. In Eqn. (ii) proposed by Ozbakkaloglu and Saatcioglu (2004), the coefficients α_1 and β_1 of the Eqn. (i) are modified so that the equation can be applied to concrete columns of strengths from normal to high-strength. Using this Eqn. (ii), the experimental shear strength values during the first and second peak of F_c 120 MPa specimens can be evaluated to be nearly on the safe side. However, the safety factor of the experimental shear strength values for F_c 120 MPa specimens during the second peak is comparatively low with respect to that of F_c 80 MPa specimens.

It is assumed that the ultimate compressive strain at extreme fiber (ε_u) is 0.003 in the flexural capacity calculation method using these rectangular stress blocks. This is the reason why it is not suitable for calculating the shear strength during the second peak (flexural capacity) where the high-strength longitudinal reinforcements of a column undergo compressive yield phenomenon as observed in this study.

5. CONCLUSIONS

A bending shear force test was conducted on RC and PCa columns with ultra-high-strength materials subjected to varying axial load, and the following findings were obtained:

1. With almost equal calculated flexural strength provided for specimens with longitudinal reinforcements D22(# 7) (SD490) and D19(# 6) (USD685), the former developed spalling of cover concrete immediately after the compressive yield of longitudinal reinforcements, while the latter first developed spalling of cover concrete and then compressive yield of longitudinal reinforcements.
2. Specimens with a concrete design nominal strength of F_c 80 MPa and F_c 120 MPa were subjected to a load of compressive axial force of $0.55F_cbD$ and $0.50F_cbD$ respectively. The axial strains during large story drift angle in the F_c120 MPa specimen was larger than that in the F_c 80 MPa specimen, while spalling of cover concrete developed widely in the F_c 120 MPa specimen.
3. PCa column specimens of both F_c 80 MPa and F_c 120 MPa indicated larger shear strength during cover concrete spalling than RC column specimens. On the contrary, an increase in shear strength thereafter was small. The maximum shear strength of PCa column specimens was also a little lower than that of the RC column specimens prepared by monolithic casting.
4. The flexural capacity of each specimen was evaluated by the rectangular stress block method in compliance with Building Code and Commentary ACI 318-02 (2002). The flexural capacity levels obtained with F_c 80 MPa specimens were largely on the safe side, whereas those obtained with F_c 120 MPa were not necessarily on the safe side. However, it was confirmed that the experimental values were considered to be on the safe side by applying the stress blocks in accordance with the proposal of Ozbakkaloglu and Saatcioglu (2004) to the evaluation.

NOTATION

A_c = area of core concrete within perimeter hoop (center-to-cente), A_g = gross area of column cross-section,
A_{st} = total area of longitudinal reinforcement,
b = width of a column cross-section, D = overall depth of a column cross-section
F_c = design nominal strength of concrete, f_c' = concrete cylinder compressive strength,
f_y = yield strength of longitudinal reinforcement,
P = axial load, P_0 = nominal concentric compressive capacity of a column calculated according to Eqn. 3.1,
$P_{0(HSC)}$ = nominal concentric compressive capacity of a column using concrete of strength from normal to high strength level (120 MPa) calculated according to Eqn. 3.2,
α_1 = coefficient that defines width of rectangular stress block, β_1 = coefficient that defines height of rectangular stress block, ε_u = extreme copression fiber strain in concrete at ultimate moment resistance,
γ = coefficient defined in Eqn. 3.4

REFERENCES

ACI Committee 318, (2002). Building Code Requirement for Structural Concrete (ACI 318-02) and Commentary (318R-02), American Concrete Institute, Farmington Hills, Mich.

Ozbakkaloglu, T., and Saatcioglu, M. (2004). Rectangular stress block for high-strength concrete, *ACI Structural Journal* **101:4**, 475-483.